International Journal of Biological Macromolecules 318 (2025) 145094

Contents lists available at ScienceDirect

International Journal of Biological Macromolecules

journal homepage: www.elsevier.com/locate/ijbiomac

Molecular and structural changes in starch and proteins induced by microwave treatment and their effect on pasting properties. A study on amaranth, buckwheat, quinoa, and sorghum in grain and flour form

Ainhoa Vicente [a,b], Raúl R. Mauro [a,b], Marina Villanueva [a,b], Pedro A. Caballero [a,b], Bruce Hamaker [c], Felicidad Ronda [a,b,*]

[a] Department of Agriculture and Forestry Engineering, Food Technology, College of Agricultural and Forestry Engineering, University of Valladolid, Av. Madrid, 44, 34004 Palencia, Spain
[b] Research Institute on Bioeconomy - BioEcoUVa, PROCEREALtech Group, University of Valladolid, Spain
[c] Whistler Center for Carbohydrate Research, Department of Food Science, Purdue University, West Lafayette, IN, USA

ARTICLE INFO

Keywords:
Asymmetric flow field-flow fractionation
Size-exclusion chromatography
Confocal scanning laser microscopy
Pasting properties
Microwave treatment

ABSTRACT

This study investigated the effects of microwave treatment (MWT) on the molecular structure and properties of starch and proteins, as well as on the pasting properties of flours. MWT was performed under uniform conditions (25 % moisture, 100 °C, 30 min) for amaranth, buckwheat, quinoa, and sorghum in two forms: grain and flour. MWT generally caused fragmentation of amylose and amylopectin, reducing amylopectin molar mass by up to 39 % and amylose long chains by up to 18 %, disrupting protein secondary structure (α-helix content up to −5 %), and altering morphology of starch granules and protein. All flours presented an orthorhombic crystal structure that was maintained after MWT. MWT changes were generally more pronounced in flour than in grain treatments, with amaranth showing the greatest change and buckwheat the least. Microwave-induced changes in pasting properties depended on intrinsic flour properties and structural modifications. Principal component analysis revealed a consistent change in all treated samples, but to varying degrees depending on botanical origin and treatment form. This study contributes to a deeper understanding of structural changes of starch and proteins by MWT and their contribution to altered pasting properties depending on whether the treatment is applied to grain or flour.

1. Introduction

There is a growing interest in the use of alternative grains as main ingredients in cereal-based foods, particularly those with high intrinsic nutritional or health-related value, such as amaranth, buckwheat, quinoa, and sorghum [1,2]. These matrices exhibit differences in proximate composition and structure of their main biopolymers, namely, starch and protein. Starch is the main component of these flours, typically ranging from 55 to 65 % for amaranth, 54 to 72 % for quinoa, 68 to 78 % for buckwheat, and 55.6 to 70 % for sorghum (referred to as dry matter) [1,3,4]. Starch is located in the endosperm as granules of different sizes: 0.5–2 μm for amaranth, 1–2 μm for quinoa, 2–15 μm for buckwheat and 5–30 μm for sorghum [5]. All these matrices have an A-type diffraction pattern of starch [4]. Protein is the second major component in these matrices, ranging from 13 to 22 % for amaranth, 9–17 % for quinoa, 6–15 % for buckwheat, and 7–15 % for sorghum (referred to dry matter) [1,6]. The main proteins in sorghum are prolamins, primarily located in the endosperm, whereas in amaranth, quinoa, and buckwheat the predominant proteins are globulins, which are more concentrated in the embryo [1,6].

Native starches and flours often have limited functionality, which affects the sensory and textural properties of final products, depending on the composition and the interaction of the components during food processing [3,7,8]. Consequently, various techniques have been developed to modify the functionality of starch and flour to better align them with the requirements of the food industry, including physical, chemical, and enzymatic modifications [7,9]. Heat moisture treatment (HMT) is a physical modification that has been widely applied to modify the

* Correspondence to: F. Ronda, Department of Agriculture and Forestry Engineering, Food Technology, College of Agricultural and Forestry Engineering, University of Valladolid, Av. Madrid, 44, 34004 Palencia, Spain.
E-mail address: mfronda@uva.es (F. Ronda).

https://doi.org/10.1016/j.ijbiomac.2025.145094
Received 11 December 2024; Received in revised form 26 May 2025; Accepted 7 June 2025
Available online 8 June 2025

functionality of starch [9,10]. This method involves subjecting starch to high temperatures (above the glass transition temperature) but limiting the moisture content (typically 10–30 %) to avoid or minimise its gelatinisation [11]. HMT has been demonstrated to be effective in producing structural modifications of amylose and amylopectin that change functionality, i.e., rheological, pasting, and thermal characteristics of starches [9].

Microwave treatment (MWT) has been proposed as an interesting alternative technique to perform HMT, as microwave radiation produces a faster heating of the sample, reduces energy consumption, and offers greater efficiency [12]. MWT is an effective method for modifying starch structure, resulting in the formation of cracks and a rough surface on the starch granules, alterations in crystallinity and crystal type, rearrangements in crystalline and amorphous regions, and a reduction in its molecular mass and short-range molecular order [7,12,13]. Changes in molecular structure of starch subjected to thermal modifications have been studied using various techniques, including Fourier transform infrared spectroscopy (FTIR), nuclear magnetic resonance (NMR), size-exclusion chromatography (SEC) coupled with different detectors, and high-performance anion exchange chromatography-pulsed amperometric detection (HPAEC-PAD) [9,13]. The commonly used HPSEC technique presents limitations in accurate determination of amylopectin structure due to possible shear scission of this highly branched polymer [14]. Asymmetric flow field-flow fractionation (AF4) is a powerful separation technique for characterising amylopectin because it preserves its integrity and structure [4,14]. This technique has been used to characterise native starches; however, to the best of our knowledge, it has not yet been used to determine the impact of MWT.

As extracted from the reviews by Yi et al. [12] and Zhao et al. [7], most studies on MWT have focused on the treatment of individual components, mainly starch, particularly when evaluating structural modifications. The trend to use wholemeal grains/flours for the production of clean label and nutritious-dense food products makes it important to assess the effect of MWT when performed on whole flours and grains instead of isolated starches. The different components, mainly starch and protein, present in these matrices may interact during MWT, potentially leading to different structural and functional modifications [15]. Recent studies have evaluated the MWT of more complex grain matrices, including different grains or flours of cereals and pseudocereals [5,15–20]. These studies identified a significant impact of the treatment conditions (power, frequency, temperature, time, moisture, etc.) and the botanical origin of the sample on the modification of its properties, as previously reported for starch. Although most studies on MWT have been performed on flours, the treatment of the whole grains prior to milling presents several advantages, particularly in terms of processing and long-term storage, as grains are relatively resistant to deterioration during preservation [16]. The grain treatment simplifies the process, improves homogeneity, and eliminates the risk of handling powdery systems [21]. It has also been reported that the use of grains instead of flour in MWT results in different water mobility and distribution during heating, leading to variations in thermal properties, colour, and functional properties such as water absorption and emulsifying capacity [5]. However, the differential effects of MWT on the structural properties of grain treatment versus flour treatment remain underexplored. Understanding how MWT alters the structure of flour components depending on their initial characteristics and how these modifications influence pasting behaviour is crucial for elucidating the structure-function relationships in MWT-induced modifications.

This study aimed to investigate the structural modifications of starch and protein by MWT and their contribution to modified pasting properties. For this aim, four matrices of different botanical origins (amaranth, buckwheat, quinoa, and sorghum) and two treatment forms (grain and flour) were evaluated. The findings of this study will contribute to a deeper understanding of the effect of MWT on pasting properties in relation to the structural modifications of starch and proteins in complex matrices.

2. Materials and methods

2.1. Raw materials

Amaranth grains (*Amaranthus* spp.) were purchased on the local market, dehulled buckwheat grains (*Fagopyrum esculentum* Moench) of the Kora variety were obtained from Grupa Producentów Ekologicznych Dolina Gryki Sp ZOO (Miedzylesie, Poland), quinoa grains (*Chenopodium quinoa* Willd.) of the Vegarosa variety were provided by Herba Ricemills (Sevilla, Spain), and sorghum grains (*Sorghum bicolor* L. Moench) were provided by Salutef (Palencia, Spain). The proximate composition of the matrices used in this study (amaranth, buckwheat, quinoa, and sorghum) was previously reported by Vicente et al. [5].

2.2. Microwave treatment (MWT)

To obtain the untreated/native flours, the native grains of amaranth, buckwheat, quinoa, and sorghum were ground in a hammer mill (LM 3100, Perten Instruments, Stockholm, Sweden) with a 500 μm mesh. The moisture content (MC) of the flours and grains was determined following the official AACC method 44–15.02 (AACC, 2010). The native grains and flours were subsequently hydrated to attain a MC of 25 % by incorporating distilled water while mixing and allowing equilibration for 24 h [21]. The MC of 25 % and the treatment conditions were selected based on previous studies and preliminary tests to achieve structural changes without completely disrupting the starch and protein [21]. MWT was carried out at 900 W and 2450 MHz using a customised microwave oven (R342INW, SHARP, Japan). The microwave was equipped with a computer-controlled system to regulate the microwave application pattern and time according to the following specifications: the programmed temperature was 100 °C, with a gradual temperature increase from ambient temperature (22 ± 2 °C) to this value in 5 min, followed by 25 min of maintenance at 100 ± 3 °C. The treatment was conducted on a 250 ml hermetic and heat-resistant borosilicate glass container containing 120 ± 0.05 g of grain or flour. Additionally, a temperature data logger (Pico VACQ, TMI-Orion, Castelnau-le-Lez, France) was placed within the vessel in direct contact with the sample to record the temperature evolution during treatment. The obtained flour and grain samples were dried at 35 °C to ~12 % MC. Subsequently, the treated grains were milled in a hammer mill (LM 3100, Perten Instruments, Stockholm, Sweden) to obtain the flour, and the treated flours were disaggregated using stone mill Fidibus Medium (Komo, Hopfgarten, Austria). Each treatment was conducted in triplicate. The samples were named according to the type of MWT: untreated-native (UN), treated in the form of grain (TG), or treated in the form of flour (TF), followed by the matrix: amaranth (A), buckwheat (B), quinoa (Q), or sorghum (S). This resulted in the generation of 12 samples to be characterised.

2.3. Asymmetric flow field-flow fractionation (AF4-MALS-dRI)

Starch was isolated from the flours according to the method described by Syahariza et al. [22] with slight modifications. Briefly, flour containing the desired amount of starch (50 mg) was incubated for 30 min at 37 °C for 30 min with a protease solution (0.2 U/mg starch) in tricine buffer (250 mM, pH 7.5), and subsequently, in sodium bisulfite solution (0.45 % w/w). The precipitate was dissolved in 1.5 ml of dimethyl sulfoxide (DMSO, HPLC grade, 99.9 %) in an incubation thermal shaker (ISTHBLCTS, Ohaus, Parsippany, NJ, USA) at 80 °C for 24 h. Samples were then precipitated twice with 10 ml of absolute ethanol to obtain isolated starch, transferred to an 11 ml glass container, freeze-dried, and stored in a desiccator. Immediately prior to analysis, the isolated starch samples were solubilised by the addition of 3 ml of DMSO and stirred for 1 h at 100 °C. Subsequently, the sample was diluted with the carrier liquid to a final concentration of 1 mg/ml and stirred for 5 min at 100 °C.

The isolated starch samples were fractionated and characterised using asymmetric flow field-flow fractionation (AF4) (Eclipse WEC-04, Wyatt Technology, Santa Barbara, CA, USA) connected to an online multi-angle light scattering (MALS) (Dawn WD3–04, Wyatt Technology) and a differential refractive index (dRI) detector (Optilab WOP1–03, Wyatt Technology), both operating at 658 nm. The fractionation channel was a long channel (LC400WL, Wyatt Technology, Santa Barbara, CA, USA) with trapezoidal geometry and a nominal height of 400 μm. The ultrafiltration membrane forming the accumulation wall was a regenerated cellulose membrane with a nominal cut-off of 10 kDa (Merck Millipore). The performance of the AF4 system was evaluated using bovine serum albumin (BSA) (Sigma Aldrich, St. Louis, MO, USA) solution (1 mg/ml, w/v). The carrier liquid was deionised water containing 10 mM $NaNO_3$ and 200 ppm NaN_3 [4]. An isocratic pump (Agilent 1260 Infinity II, Agilent Technologies, Waldbronn, Germany) with a vacuum degasser was used to deliver the carrier flow. Sample injection was performed with an auto-sampler (Agilent 1260 Infinity II), injecting 120 μg of the sample into the channel at a flow rate of 0.2 ml/min. The analysis was performed using a channel flow rate of 0.6 ml/min and a detector flow rate of 0.3 ml/min. After the injection, focussing/relaxation was performed at a constant cross-flow of 3.5 ml/min for 5 min. The crossflow rate was programmed to decay linearly from 3.5 ml/min to 0 ml/min in 25 min. The total duration of each run was 60 min. An identical assay was conducted using a blank, the profile of which was used to subtract the baseline from the dRI. Data were processed using ASTRA software (*v*. 8.1.2.1, Wyatt Technology, Santa Barbara, CA, USA). M_w (weight-average molar mass), M_n (number-average molar mass), Đ (dispersity), and R_z (z-average root-mean-square radius) distributions were calculated using the first-degree fit of the Berry method [23,24]. The second virial coefficient (A2) was neglected, and a specific refractive index (dn/dc) of 0.151 ml/g was used [25].

2.4. Size-exclusion chromatography (SEC-dRI)

The chain-length distribution of debranched starches was analysed in duplicate using an Agilent 1260 size exclusion chromatography (SEC) system (Agilent Technologies, Santa Clara, CA, USA) equipped with a dRI (Optilab, Wyatt Technology, Santa Barbara, CA, USA). A set comprising GRAM pre-column, GRAM 100, and GRAM 1000 analytical columns (PSS GmbH, Mainz, Germany) connected in series was used for analysis. The carrier liquid was a solution of DMSO containing 0.5 % (w/w) LiBr at a flow rate of 0.6 ml/min and temperature of 70 °C [14,26,27]. Starch was isolated from the flours in accordance with the methodology described in Section 2.3 [22]. However, only 6 mg of starch was weighed. Furthermore, following the precipitation of starch with ethanol, a debranching reaction was conducted by dissolving the starch in 0.9 ml of warm water, adding 0.1 ml of acetate buffer (0.1 M, pH 3.5), 5 μl of sodium azide solution, and 2.5 μl of isoamylase (Megazyme, Wicklow, Ireland), and incubating at 37 °C for 3 h [27]. The samples were then freeze-dried to obtain the dried debranched starch.

Pullulan standards (PSS GmbH, Mainz, Germany) with molecular weights ranging from 342 to 6.36×10^5 were employed for calibration purposes. This enabled the conversion of the elution volume to hydrodynamic volume (V_h) in accordance with the Mark-Houwink equation, with the parameters $K = 2.424 \times 10^{-4}$ dl/g and $\alpha = 0.68$ [14], and was converted into the degree of polymerisation (DP) [28]. The SEC weight distributions, w(log Vh), were obtained from the dRI signal and plotted as a function of DP. To enable more accurate comparisons between treatments, all samples were normalised to yield the same area under the curve (AUC). The amylose (AM) ratio was calculated as the AUC of the amylose peak (DP $\geq$ 100) divided by the total AUC of both the amylopectin (AP) and AM peaks [26,27]. Amylose chain-length distributions (CLD) were divided into three regions: short chains (AM1: DP $\sim$ 100–300), medium chains (AM2: DP $\sim$ 300–1600), and long chains (AM3: DP > 1600) [26,27]. Subsequently, the amylose region was fitted to individual peaks by iterative fitting, assuming Gaussian band shapes, using OriginPro 2023 (OriginLab Corporation, Northampton, MA, USA). The amount corresponding to each region was determined as the AUC of the region divided by the total AUC of the three regions, allowing for a better quantitative comparison of amylose structural differences. Amylopectin chains were divided into two categories: short branches (AP1) and long branches (AP2). The positions of the peaks (X_{AP1} and X_{AP2}) and the height ratio (h_{AP2}/h_{AP1}) were calculated using a previously reported method [27].

2.5. Fourier transform infrared (FTIR) spectroscopy

Infrared (IR) spectra of the flour samples (equilibrated at 6 % MC) were recorded using a nitrogen-cooled FTIR spectrometer (Nicolet Nexus 670, Thermo Fisher Scientific, Madison, WI, USA) equipped with an attenuated total reflectance (ATR) accessory. Spectra were obtained between 4500 and 800 cm^{-1} at resolution of 4 cm^{-1}, and 36 scans were performed. Amide *I* peak (1700–1600 cm^{-1}) was studied to analyse the secondary structure of the protein, as described by Ozturk et al. [29] and Fevzioglu et al. [30]. The spectra were subjected to autobaseline correction, the Amide *I* peak was deconvoluted (half-bandwidth of 30 and enhancement factor of 3), and a curve-fitting procedure assuming Gaussian band shapes was performed using OMNIC software (Thermo Fisher Scientific, Madison, WI, USA). The integrated areas were used to calculate the relative amounts of protein secondary structures from the assigned bands in the spectrum: high-frequency β-sheet (1700–1690 cm^{-1}), β-turns (1690–1665 cm^{-1}), α-helix (1665–1650 cm^{-1}), random coil (1650–1640 cm^{-1}), low-frequency β-sheet (1640–1615 cm^{-1}), and side chains (1615–1600 cm^{-1}) [30,31]. The region between 1065 and 950 cm^{-1}, located within the starch fingerprint region (1200–800 cm^{-1}), was analysed as it contains vibrational bands associated with the molecular organization of starch. Four replicates were analysed for each sample.

2.6. X-ray diffraction (XRD)

A Bruker-D8-Discover-A25 diffractometer (Bruker AXS, Rheinfelden, Germany) was employed for XRD analysis, equipped with a CuKα radiation (λ = 0.154 nm) operating at 40 kV and 30 mA. Samples were equilibrated to 15 % humidity using an incubation chamber (Memmert ICP260, Schwabach, Germany) at saturated humidity and 15 °C prior to analysis. The diffraction patterns and relative crystallinity were obtained in the range of 5–40° (2θ) at a rate of 1.2°/min. The scan step size was 0.02°, the divergence slit width was 1°, and the scatter slit width was 2.92°.

2.7. Confocal laser scanning microscopy (CLSM)

Carbohydrates were labelled using the periodic acid-Schiff (PAS) reaction [32], and proteins were labelled with fluorescamine [33] in accordance with the procedure described by Ozturk et al. [29]. 20 mg of flour was oxidised with 0.5 % (v/v) periodic acid for 5 min, rinsed three times with deionised water, and then 500 μl of Schiff reagent was added and allowed to stain for 10 min. Subsequently, the samples were rinsed twice with 0.5 % (v/v) potassium sulfite and five times with deionised water. Samples were then treated for protein labelling with 200 μl of 0.1 % (w/v) fluorescamine in acetonitrile and 300 μl of 0.1 M sodium (tetra) borate buffer (pH 8.0) for 5 min and rinsed five times with deionised water. Following each step, the samples were centrifuged at 13,000 rpm for 5 min and the supernatant was removed. 0.1 ml of 75 % (v/v) glycerol solution was added to ensure the stability of labelling. 10 μl of the stained samples was placed on microscope slides, and coverslips were adhered using nail varnish. Samples were examined using a confocal laser scanning microscope (LSM 880, Carl Zeiss Microscopy, Oberkochen, Germany) equipped with an air-cooled 10 mW output Krypton/Argon laser (ILT Laser, Bio-Rad Laboratories, Hercules, USA), a water-cooled Innova Enterprise 60 mW output Argon ion laser

Table 1
Starch structural parameters of flour samples obtained from untreated and microwave-treated flours and grains.

Sample	AF4-MALS-dRI						SEC-dRI				
	AM M_W (10^6 g/mol)	AM r_z (nm)	AM Đ	AP M_W (10^8 g/mol)	AP r_z (nm)	AP Đ	AM ratio (%)	AUC_{AM1} (%)	AUC_{AM2} (%)	AUC_{AM3} (%)	h_{AP2}/h_{AP1}
UN-A	6.4 ± 0.3 a	44 ± 3 a	1.09 ± 0.01 a	10.6 ± 0.8 c	387 ± 4 c	3.5 ± 0.7 b	2.4 ± 0.1 a	nd	nd	nd	0.594 ± 0.006 b
TF-A	14.0 ± 2.0 b	96 ± 8 b	1.21 ± 0.02 a	6.5 ± 0.4 a	290 ± 3 a	2.1 ± 0.2 a	1.8 ± 0.2 a	nd	nd	nd	0.578 ± 0.006 a
TG-A	24.7 ± 3.0 c	134 ± 5 c	1.22 ± 0.17 a	8.0 ± 0.6 b	326 ± 19 b	2.3 ± 0.4 a	1.9 ± 0.5 a	nd	nd	nd	0.594 ± 0.002 b
UN-B	3.1 ± 0.1 a	52 ± 3 b	1.03 ± 0.01 a	2.5 ± 0.1 a	207 ± 3 a	1.4 ± 0.1 ab	30.8 ± 1.4 a	18.1 ± 0.4 a	44.5 ± 0.4 a	37.5 ± 0.1 b	0.617 ± 0.004 a
TF-B	5.5 ± 0.5 b	71 ± 6 b	1.08 ± 0.02 b	2.5 ± 0.1 a	196 ± 8 a	1.4 ± 0.1 a	31.7 ± 1.4 a	20.6 ± 0.2 c	45.0 ± 0.1 a	34.5 ± 0.4 a	0.641 ± 0.008 b
TG-B	3.6 ± 0.5 a	58 ± 9 ab	1.07 ± 0.02 b	2.4 ± 0.1 a	201 ± 6 a	1.3 ± 0.1 b	31.5 ± 1.1 a	19.6 ± 0.1 b	45.3 ± 0.4 a	35.2 ± 0.4 a	0.631 ± 0.003 ab
UN-Q	3.5 ± 0.2 a	38 ± 6 a	1.22 ± 0.04 a	8.1 ± 0.2 c	354 ± 2 c	4.7 ± 0.2 c	22.9 ± 0.6 a	29.3 ± 0.4 a	48.6 ± 0.4 a	22.2 ± 0.7 c	0.622 ± 0.004 a
TF-Q	4.8 ± 1.1 a	70 ± 7 b	1.22 ± 0.12 a	5.7 ± 0.3 a	282 ± 4 a	2.8 ± 0.1 a	21.9 ± 0.4 a	31.8 ± 0.3 b	50.1 ± 0.2 b	18.2 ± 0.1 a	0.616 ± 0.001 a
TG-Q	4.0 ± 0.6 a	66 ± 7 b	1.24 ± 0.07 a	7.2 ± 0.3 b	312 ± 7 b	3.3 ± 0.3 b	22.5 ± 1.4 a	30.7 ± 0.6 b	49.2 ± 0.2 a	20.3 ± 0.8 b	0.619 ± 0.005 a
UN-S	4.8 ± 0.1 a	67 ± 7 a	1.18 ± 0.06 a	2.3 ± 0.2 b	185 ± 10 b	1.5 ± 0.2 a	32.7 ± 0.8 a	21.9 ± 1.3 a	42.3 ± 0.3 ab	35.8 ± 1.0 b	0.542 ± 0.006 a
TF-S	4.5 ± 0.4 a	68 ± 5 a	1.29 ± 0.05 b	2.0 ± 0.1 a	174 ± 3 a	1.6 ± 0.2 a	32.7 ± 0.6 a	22.3 ± 0.1 a	41.6 ± 0.4 a	36.2 ± 0.5 b	0.540 ± 0.001 a
TG-S	4.3 ± 0.4 a	66 ± 4 a	1.27 ± 0.02 b	2.1 ± 0.1 ab	188 ± 4 b	1.5 ± 0.1 a	33.6 ± 0.1 a	24.9 ± 0.4 b	42.7 ± 0.1 b	32.5 ± 0.5 a	0.555 ± 0.006 a
Analysis of variance and significance (*p-values*)											
Matrix (F1)	***	***	***	***	***	***	***	***	***	***	***
Treatment (F2)	***	***	*	***	***	***	ns	***	*	***	*
F1 × F2	***	***	ns	***	***	***	ns	**	**	**	**

Flours obtained from untreated-native (UN), microwave-treated grain (TG), and microwave-treated flour (TF) samples of amaranth (A), buckwheat (B), quinoa (Q), and sorghum (S). AM: amylose, AP: amylopectin, M_w: weight-average molar mass, M_n: number-average molar mass, r_z: z-average root-mean-square radius, Đ: dispersity calculated as M_w/M_n. AM ratio: area under the curve of amylose peak related to the total area of amylose and amylopectin. AUC_{AM1}, AUC_{AM2}, AUC_{AM3}: percentual area under the amylose peak corresponding to short, intermediate, and long amylose chains, respectively. X_{AP1}, X_{AP2}: degree of polymerisation (DP) of the maximum peak for short and long amylopectin chains, respectively. h_{AP2}/h_{AP1}: height ratio of AP2 to AP1. nd: non-detectable. Data are expressed as mean ± standard deviation. Significant statistical differences ($p < 0.05$) are indicated by different letters for the same parameter and matrix. Analysis of variance and significance of matrix (A,B,Q,S), treatment (UN, TG, TF), and their interaction: ***$p < 0.001$, **$p < 0.01$, *$p < 0.05$, ns: non-significant.

(Coherent Inc., Santa Clara, USA), three fluorescence detection channels, and various lenses (20× and 63×). The excitation and emission wavelengths for carbohydrates were 488 nm and 590/60 nm, respectively, while those for proteins were 405 nm and 450/80 nm, respectively [29]. The pinhole size was set to 1 AU, and images were recorded as Z-stacks incorporating the visible range of each sample using the Zen BLACK software (Carl Zeiss imaging, Oberkochen, Germany). Image analysis and 3D image formation were conducted using Zen Blue software (Carl Zeiss imaging, Oberkochen, Germany).

2.8. Pasting properties

Flour pasting properties were determined using a Rapid Visco Analyser (RVA) model 4500 (Perten Instruments, Stockholm, Sweden) in duplicate. A mixture of 3.5 g of flour (14 % MC) with 25 ml of water was prepared, and the Standard 1 temperature profile of AACC official method 76-21.01 [34] was used. The following parameters were calculated from the pasting curve: pasting temperature (PT), peak viscosity (PV), trough viscosity (TV), breakdown viscosity (BV), final viscosity (FV), and setback viscosity (SV).

2.9. Statistical analysis

The statistical analysis was performed using Statgraphics Centurion 19 software (Bitstream, Cambridge, MN, USA). Significant differences between samples ($p < 0.05$) were assessed using an analysis of variance (ANOVA) with the least significant difference (LSD) test. The results were reported as the mean values of different replicates, accompanied by the standard deviation. Additionally, a multivariate analysis of variance (MANOVA) study was conducted to examine the effects of the studied factors: the matrix (amaranth, buckwheat, quinoa, and sorghum) and the MWT (untreated-native flour, microwave-treated grain, and microwave-treated flour), as well as their interactions. Principal component analysis (PCA) was performed using OriginPro 2024 (Northampton, MA, USA).

3. Results and discussion

3.1. Starch molecular structure

The molecular structure of the starch samples was studied using AF4-MALS-dRI for the whole starch molecules, and SEC-dRI for debranched starch molecules. A summary of the results of both analyses is provided in Table 1. Fig. 1 shows the fractograms obtained from the AF4-MALS-dRI. For each matrix, the MALS signal at a 90° scattering angle and the calculated molar mass profiles for the native and the two treated samples are presented to highlight the effect of treatment on the molar mass profile. In addition, Supplementary Fig. 1 presents the complete data for each sample, including the MALS and dRI signals and the calculated molar mass and radius profiles. The fractograms were divided into three zones corresponding to three fractions of starch molecules according to their molecular mass and radius profiles: a) a fraction related to the molecules of the highest molecular weight and size with the main peak in the MALS signal that corresponded to amylopectin

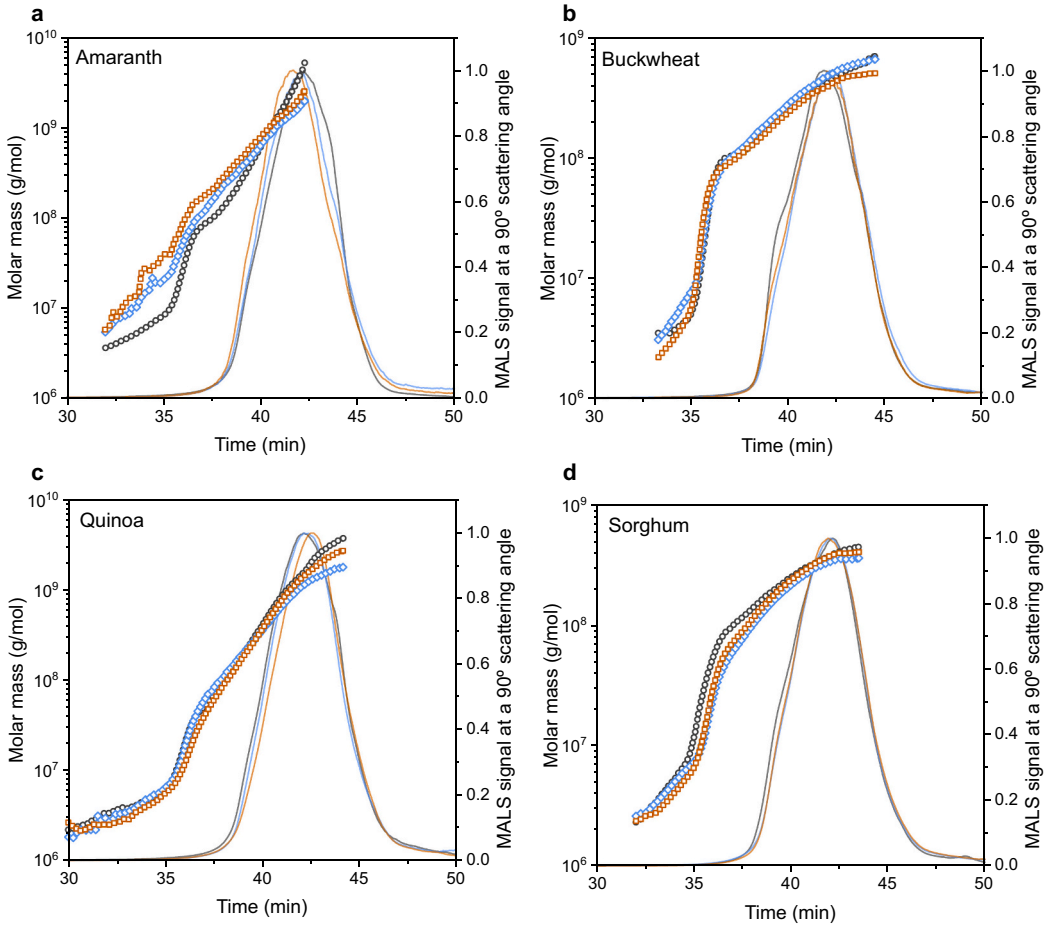

Fig. 1. Fractograms from AF4 showing molar mass (left axis) determined by MALS-dRI detection (symbols) and MALS signal at a 90° scattering angle (right axis) (lines) of amaranth (a), buckwheat (b), quinoa (c), and sorghum (d). In each graph, untreated-native flour (black, circle) is compared with microwave-treated flour (blue, diamond) and microwave-treated grain (brown, square).

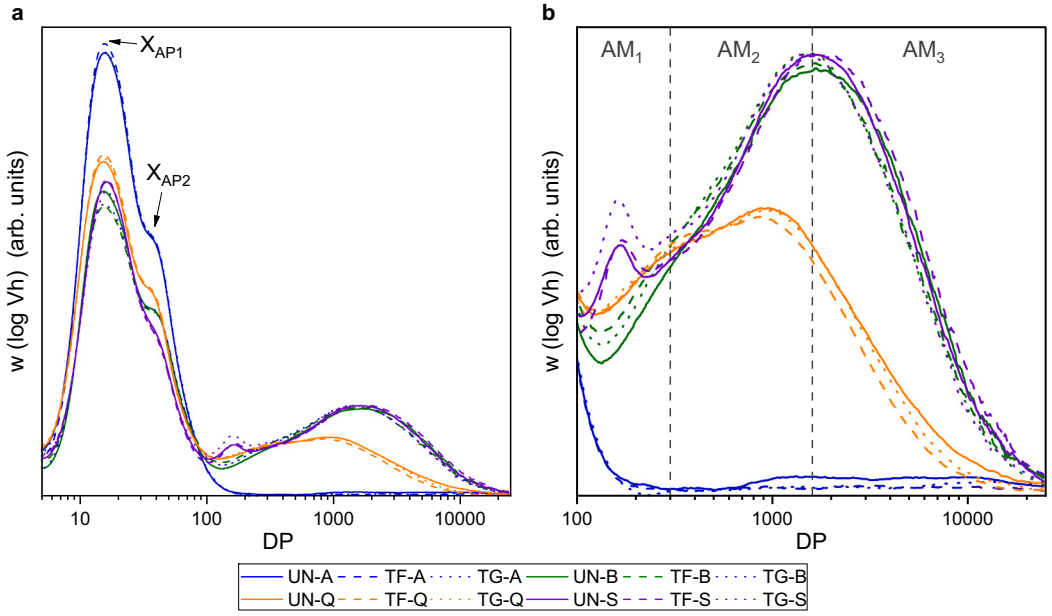

Fig. 2. Size exclusion chromatograms of debranched starch samples (a) with enlargement of amylose regions (b) as a function of the degree of polymerisation (DP). Untreated-native flour (UN), microwave-treated grain (TG), and microwave-treated flour (TF) from amaranth (A), buckwheat (B), quinoa (Q), and sorghum (S).

molecules (amylopectin zone) b) a second fraction related to amylose molecules, which eluted earlier, in the region between ~10 min and 20–30 min (depending on the starch) (amylose zone), and c) an intermediate fraction between the other two of unresolved high-molecular-weight amylose and low-molecular-weight amylopectin (intermediate zone) not taken into account in the calculations.

Amaranth displayed the largest amylopectin size among the native starches studied (weigh-average molar mass, M_w, of $1{\cdot}10^9$ g/mol), followed by quinoa (M_w of $8{\cdot}10^8$ g/mol), buckwheat (M_w of $2.5{\cdot}10^8$ g/mol), and sorghum ($2.3{\cdot}10^8$ g/mol). Large amylopectin molar mass and radius values were previously reported for native amaranth starch using AF4 by Fuentes et al. [4]. The authors indicated that these sizes may have an error of up to 25 % in molar mass owing to neglecting the second virial coefficient. Furthermore, the radius size was in the upper limit of the Rayleigh–Gans–Debye light scattering theory. Therefore, the molar mass and radius values of amaranth and quinoa should be considered apparent. MWT resulted in a clear reduction in M_w and r_z (z-average root-mean-square radius) for the amaranth and quinoa samples. As illustrated in Fig. 1, treated amaranth and quinoa exhibited a reduction in molecular size at higher retention times (corresponding to larger molecules), resulting in lower M_w and r_z values than their native counterparts. This effect was amplified when the treatment was performed in flour rather than in grain form. For instance, TF-A presented a reduction of −39 % in M_w and TG-A of −25 % when compared to UN-A. Sorghum showed a similar trend, albeit to a lesser extent, with reductions of approximately 10 % for TF-S compared to UN-S. A possible explanation for the smaller effect of the grain treatment compared to the flour treatment can be attributed to the intact structure of the grain, which preserves cell integrity and limits component interactions during MWT [5,21]. In contrast, milling in flour disrupts the cells, increasing molecular interactions and facilitating starch hydrolysis. It is important to highlight that native amaranth and quinoa samples had a high degree of amylopectin dispersity (Đ), with values of 4.7 and 3.5, respectively, while sorghum and buckwheat samples had values of 1.6 and 1.4, respectively. The largest reduction in molecular mass observed in the amaranth and quinoa samples was accompanied by a decrease in Đ, suggesting that the molecules became more uniform in size because of preferential fragmentation of larger molecules.

Debranched amylopectin was studied using SEC-dRI, and the weight distributions ($w(\log V_h)$) were plotted as a function of the degree of polymerisation (DP) of the debranched linear chains (Fig. 2). The samples were normalised to yield the same total area under the curve (AUC), thus facilitating the comparison of proportional changes in the different components between samples [26]. All the samples presented a typical binomial distribution for amylopectin branches (DP < 100). The DP of the two peaks corresponded to short, AP1 (DP ~ 16), and long, AP2 (DP ~ 36), amylopectin chains. Slight significant differences ($p < 0.05$) were observed due to the use of different matrices. The peak corresponding to short chains exhibited a DP of 15.6 for quinoa, 15.7 for buckwheat, 16.0 for amaranth, and 16.6 for sorghum. The DP of the peak corresponding to the long chains was 34.7 for quinoa, 36.2 for amaranth, 36.6 for buckwheat, and 36.9 for sorghum. However, these peak positions were not significantly affected by MWT ($p > 0.05$), and the height ratio between these peaks (h_{AP2}/h_{AP1}) did not present any strong modification, with only slight variations in the treated samples. This result contrasts with the substantial variations observed in the molar mass distribution of whole amylopectin molecules analysed by AF4. As the SEC profile for linear dextrins is derived from the enzymatic hydrolysis of α-(1 → 6) bonds, MWT-induced scission likely occurs mainly at branching sites (α-(1 → 6) bonds), with non-significant modifications in debranched amylopectin chains. Previous studies already reported a greater susceptibility to hydrolysis of α-(1 → 6) glycosidic bonds during MWT, and linked it to the larger steric hindrance and stability of α-(1 → 4) glycosidic bonds [35,36]. Nevertheless, it is important to acknowledge that SEC has inherent limitations in the characterisation of the short chains of amylopectin because of the potential for inaccuracies resulting from calibration using the Mark-Houwink empirical equation at low DP [37]. Consequently, it is possible that a few of the longer amylopectin chains were broken and contributed to the lower M_w observed after MWT, although this was not detected by SEC. When Tian et al. [13] performed short-time MWT on maize starch and analysed the CLD by HPAEC-PAD, they observed a reduction in amylopectin chains with DP > 45 concomitant with an increase in chains with DP < 18, indicating the possible preferential breakdown of longer chains attributed to the backbone chains and connector chains between backbone and double helices.

Regarding the molecular mass of the amylose-associated fraction measured by AF4, the average weight of the untreated molecules ranged

from 3.1 to 6.4 × 10^6 g/mol (Table 1, Fig. 1). The MWT resulted in an apparent increase in the M_w of amylose in TF-A, TG-A, and TF-B, whereas no significant differences were observed in the remaining treated samples compared with their untreated counterparts. Furthermore, an increase in r_z was observed for the samples that exhibited an increase in M_w and for the treated quinoa samples. It is particularly noteworthy the great change in the M_w and r_z of the low molecular weight fractions for amaranth samples, with +119 % and +118 % for TF-A and +286 % and +205 % for TG-A, respectively, compared to UN-A. The increases in M_w and r_z for the amylose zone, as measured by AF4, are likely due to the presence of hydrolysed amylopectin fragments with sizes similar to those of the amylose fractions. The potential coelution of degraded amylopectin molecules with amylose was also observed by Tian et al. [13] when microwaved maize starch was analysed using SEC (whole molecule). The amorphous zones of branching sites have been shown to be more susceptible to hydrolysis than the crystalline regions because of their looser structure [7]. Given the large size and degree of branching of amaranth [4], and to a lesser extent quinoa, along with their low amylose content, these matrices may be more susceptible to the formation of hydrolysed amylopectin fragments, which are detectable in the amylose-related zone in AF4.

The amylose CLD (DP > 100) obtained using SEC-dRI for debranched molecules is shown in Fig. 2. Notably, the amylose ratio, as calculated by the relative proportion of the amylose AUC (DP > 100) to the total AUC, did not vary significantly after MWT. The amylose ratio was significantly influenced by the matrix, while the treatment form (grain or flour) had no significant effect (see Table 1). SEC has been determined as an accurate method for evaluating the CLD of amylose chains [37]. The peak presented at DP > 100, has been shown to comprise three overlapping peaks, designated AM1 (DP 100–300), AM2 (DP 300–1600) and AM3 (DP > 1600) [37]. The relative AUC of each individual peak was related to the total AUC of the amylose region to determine the relative contribution of each peak (AUC_{AM1}, AUC_{AM2}, and AUC_{AM3}). Due to the low amylose content of amaranth (AM ratio ~ 2 %), it was not possible to calculate the different amylose fractions in this sample. The remaining treated samples, with the exception of TF-S, showed an increase in AUC_{AM1} and a reduction in AUC_{AM3}. This effect was more pronounced in flour than in grain treatment for buckwheat and quinoa. The decrease in the proportion of long chains and the concomitant increase in the proportion of short chains may be attributed to the partial depolymerisation of amylose during MWT [26]. Samples with higher amylose content (sorghum and buckwheat) exhibited less variation in the amylose group proportions, most likely due to the ability of amylose to form stable single- or double-helix complexes, which limits susceptibility to heat treatment-mediated hydrolysis [38].

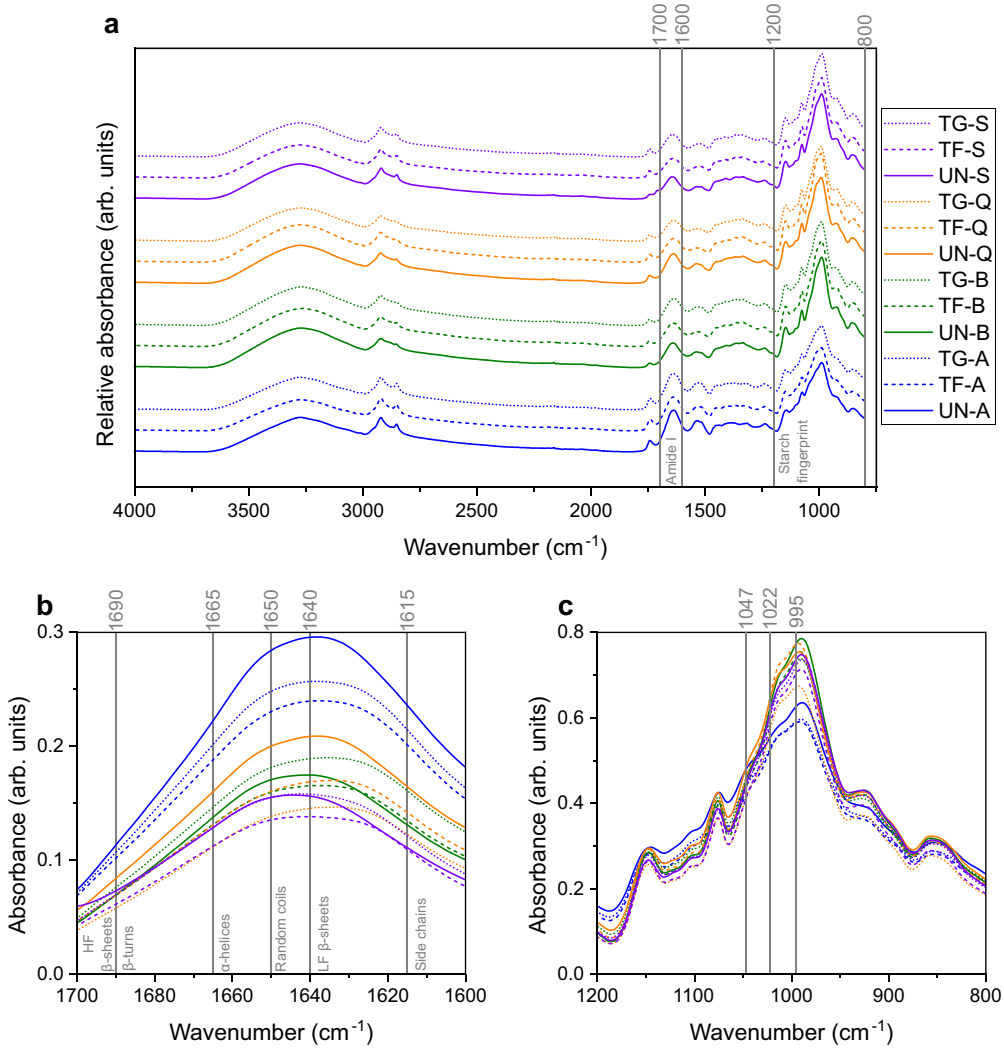

Fig. 3. Infrared (IR) spectra of untreated-native flour (UN), microwave-treated grain (TG), and microwave-treated flour (TF) from amaranth (A), buckwheat (B), quinoa (Q), and sorghum (S). Complete IR spectra (a), enlarged protein Amide *I* region (b), and enlarged starch fingerprint region (c).

Table 2
Results from X-ray diffraction and Fourier transform infrared spectroscopy analysis of flour samples obtained from untreated and microwave-treated flours and grains.

Sample	RC (%)	$I_{(031)}/I_{(231)}$	$I_{(031)}/I_{(040)}$	Side chains (%)	LF β-sheet (%)	Random coil (%)	α-helix (%)	β-turns (%)	HF β-sheet (%)
UN-A	47.2 ± 1.1 a	0.87 ± 0.02 a	1.30 ± 0.02 b	8.2 ± 0.1 a	22.8 ± 0.3 b	10.9 ± 0.4 a	25.3 ± 0.6 c	17.9 ± 0.5 a	14.8 ± 0.7 b
TF-A	48.1 ± 0.8 a	0.88 ± 0.01 a	1.24 ± 0.01 a	8.5 ± 0.1 b	21.1 ± 0.2 a	16.6 ± 0.3 c	21.5 ± 0.5 a	19.5 ± 0.3 b	12.9 ± 0.2 a
TG-A	45.6 ± 0.7 a	0.89 ± 0.01 a	1.24 ± 0.01 a	8.5 ± 0.1 b	21.1 ± 0.2 a	15.5 ± 0.6 b	22.6 ± 0.5 b	19.5 ± 0.3 b	12.7 ± 0.4 a
UN-B	44.4 ± 0.6 a	0.90 ± 0.02 a	1.27 ± 0.02 b	7.7 ± 0.1 a	20.4 ± 0.8 a	12.8 ± 0.7 a	27.8 ± 0.6 b	19.9 ± 0.4 a	11.4 ± 0.4 ab
TF-B	43.2 ± 0.9 a	0.87 ± 0.01 a	1.22 ± 0.01 a	8.1 ± 0.1 b	20.9 ± 0.4 a	12.9 ± 0.7 a	25.0 ± 0.4 a	22.1 ± 0.3 b	11.0 ± 0.3 a
TG-B	43.6 ± 0.6 a	0.87 ± 0.01 a	1.20 ± 0.01 a	8.4 ± 0.1 c	20.9 ± 0.6 a	12.7 ± 0.8 a	24.8 ± 0.4 a	21.4 ± 0.9 b	11.8 ± 0.3 b
UN-Q	46.4 ± 1.1 a	0.86 ± 0.01 a	1.33 ± 0.01 b	8.0 ± 0.1 a	22.1 ± 0.3 a	12.4 ± 0.9 a	25.3 ± 0.5 b	18.5 ± 0.5 a	13.6 ± 0.5 a
TF-Q	44.5 ± 0.6 a	0.85 ± 0.01 a	1.24 ± 0.01 a	8.6 ± 0.1 b	21.8 ± 0.4 a	17.6 ± 0.3 b	20.0 ± 0.6 a	18.3 ± 0.7 a	13.2 ± 0.1 a
TG-Q	45.4 ± 0.8 a	0.86 ± 0.01 a	1.24 ± 0.01 a	8.5 ± 0.1 b	21.9 ± 0.1 a	17.5 ± 0.5 b	20.4 ± 0.3 a	18.3 ± 0.5 a	13.3 ± 0.2 a
UN-S	47.0 ± 0.6 a	0.89 ± 0.01 a	1.24 ± 0.01 c	8.5 ± 0.2 a	24.4 ± 0.4 b	14.6 ± 0.3 a	22.1 ± 1.1 b	19.8 ± 0.7 a	11.6 ± 0.6 ab
TF-S	47.2 ± 0.8 a	0.88 ± 0.01 a	1.13 ± 0.01 a	9.0 ± 0.1 b	23.2 ± 0.3 b	17.1 ± 0.3 b	19.2 ± 0.5 a	19.8 ± 0.4 a	11.9 ± 0.1 b
TG-S	46.5 ± 0.7 a	0.86 ± 0.01 a	1.19 ± 0.01 b	8.8 ± 0.1 b	21.6 ± 1.3 a	17.4 ± 0.7 b	20.6 ± 1.2 ab	20.5 ± 0.2 a	11.2 ± 0.2 a
Analysis of variance and significance (p-values)									
Matrix (F1)	***	*	***	***	***	***	***	***	***
Treatment (F2)	ns	ns	***	***	***	***	***	***	***
F1 × F2	ns	ns	*	**	***	***	***	***	***

Flours obtained from untreated-native (UN), microwave-treated grain (TG), and microwave-treated flour (TF) samples of amaranth (A), buckwheat (B), quinoa (Q), and sorghum (S). RC: relative crystallinity. $I_{(031)}/I_{(231)}$ and $I_{(031)}/I_{(040)}$: intensity ratio between two diffraction peaks for the orthorhombic crystal structure. LF: low frequency. HF: high frequency. Data are expressed as mean ± standard deviation. Significant statistical differences ($p < 0.05$) are indicated by different letters for the same parameter and matrix. Analysis of variance and significance of matrix (A,B,Q,S), treatment (UN, TG, TF), and their interaction: *** $p < 0.001$, ** $p < 0.01$, * $p < 0.05$, ns: non-significant.

3.2. Short-range molecular order of starch and secondary structure of proteins

IR spectra were analysed to assess the vibrational changes closely related to the structural changes in the flours resulting from the MWT. The spectra of all the samples exhibited bands at similar wavenumbers. In addition, no new bands were observed to form or disappear after MWT. Nevertheless, differences in absorbance and variations in band shape were observed between samples and as a result of MWT (Fig. 3). Therefore, starch fingerprint region and Amide *I* band were evaluated to compare the aforementioned modifications in the main flour components.

Changes in the secondary structure of proteins were determined by Gaussian curve fitting after deconvolution of the Amide *I* band (1700–1600 cm^{-1}) (Fig. 3b), with the relative contributions of each protein secondary structure listed in Table 2. A significant effect ($p < 0.001$) on the relative proportion of each protein secondary structure was observed for the studied parameters (matrix and treatment form) and their interaction (matrix × treatment). MWT led to a reduction α-helix proportion in all treated samples. The α-helix, an ordered secondary structure mainly stabilized by hydrogen bonds within protein chains, reflects protein folding; therefore, its reduction may indicate modification in protein folding [39]. In addition, the other ordered structures of high-frequency and low-frequency β-sheets, were reduced in the treated amaranth and sorghum (only low-frequency β-sheets). β-Sheets are mainly stabilized by intermolecular hydrogen bonds in peptide chains, and their reduction may indicate protein aggregation [39]. These decreases in ordered structures were accompanied by increases in side chain vibrations for all treated samples in β-turns (amaranth and buckwheat) and random coils (all samples except buckwheat). These effects were similar for both grain and flour treatments, with the most notable difference observed in TF-A, which exhibited a greater increase in random coil content and a more pronounced decrease in α-helix structures compared to TG-A. These findings are consistent with previous studies reporting reduced β-sheet and α-helix proportions along with an increase in β-turns and random coils after MWT of millet flour [18] and microwave roasting of quinoa [17]. Other authors have observed increases in β-sheets with reductions in α-helix [40], or in α-helix and β-turns [16], highlighting the influence of different matrices and treatment conditions. However, a general trend towards reduced α-helix content with an increase in the proportion of disordered structures of β-turns and random coils was observed in this study and in most of the previous literature. This shift to a more disordered and flexible protein secondary structure may expose the reactive groups and enhance the reaction with other components [14–17]. Hydrothermal treatments, including MWT, have been reported to disrupt the hydrogen bonds and hydrophobic/Van der Waals forces that maintain structural stability, thus disrupting the protein secondary structure [18,40]. Furthermore, the unfolding and enhanced flexibility of the protein structure may improve protein digestibility, as reported previously for breads made with microwave-treated buckwheat [41].

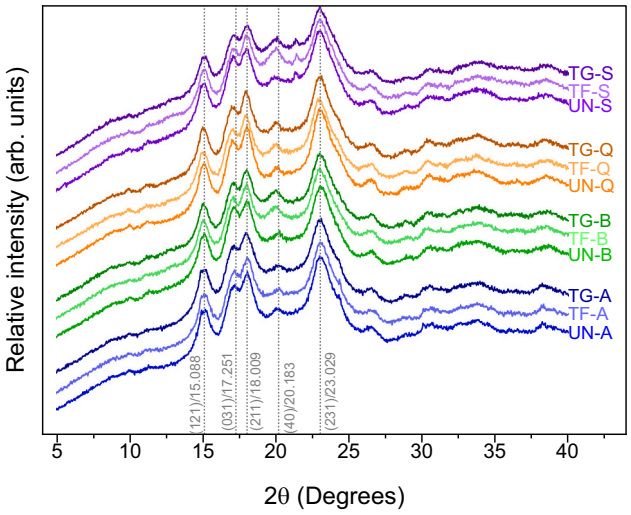

Fig. 4. X-ray diffraction (XRD) patterns of untreated-native flour (UN), microwave-treated grain (TG), and microwave-treated flour (TF) from amaranth (A), buckwheat (B), quinoa (Q), and sorghum (S). Major diffraction peaks are labelled with their corresponding Miller indices (in grey).

The starch fingerprint is presented in the region between 1200 and 800 cm^{-1} (Fig. 3c). In particular, the range from 1060 to 960 cm^{-1} has been associated with the spatial organization of starch, attributed to vibrations of the C-O-H functional groups in the polymer chains [42].

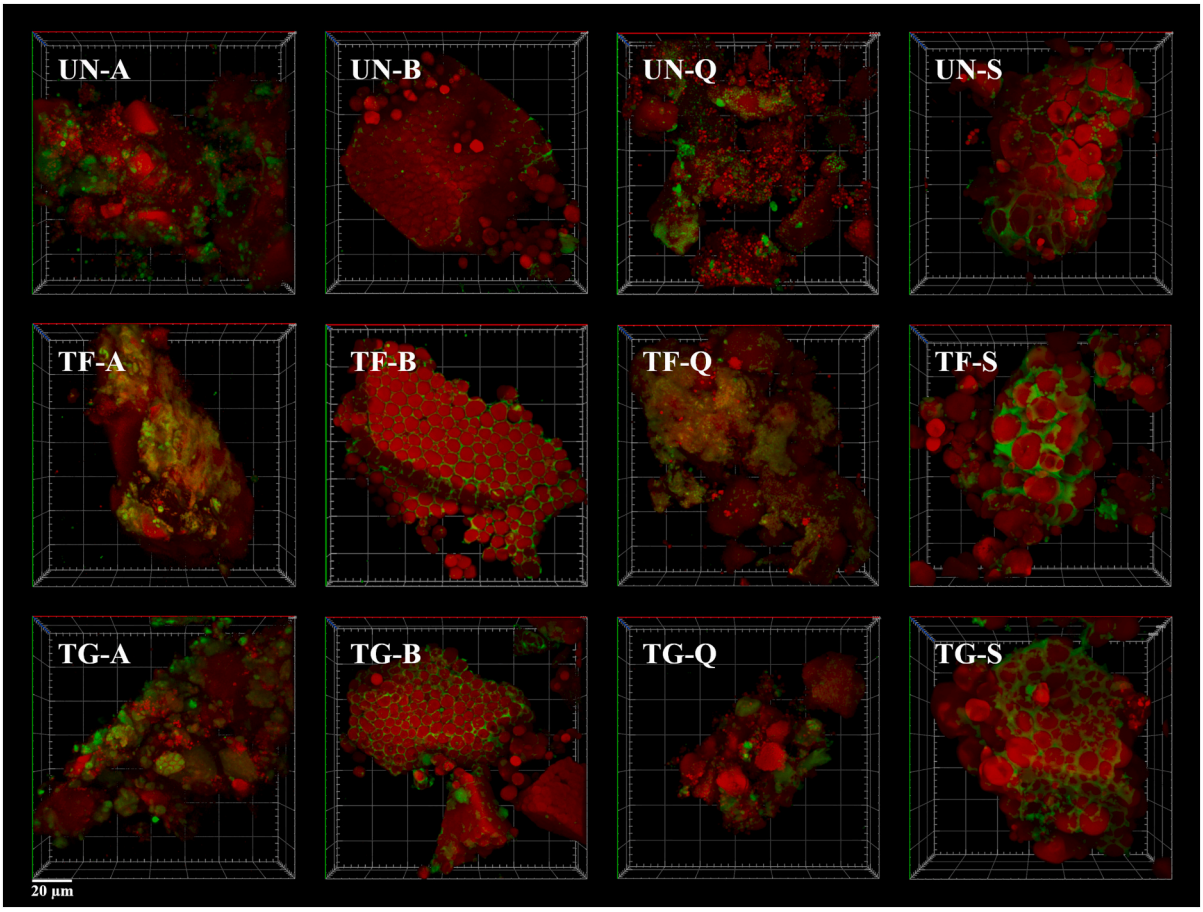

Fig. 5. Confocal laser microscopy (CLSM) images of untreated-native flour (UN), microwave-treated grain (TG), and microwave-treated flour (TF) from amaranth (A), buckwheat (B), quinoa (Q), and sorghum (S) samples at a magnification of ×63. The image shows carbohydrates in red and proteins in green, with the scale representing the main division of 20 µm.

Bands within this region are known to be sensitive to structural changes in starch, particularly those at 995, 1022 and 1047 cm^{-1} [43]. Following MWT, shifts in band position and notable changes in intensity were observed. The band near 995 cm^{-1} became broader, leading to increased overlap with the band at 1022 cm^{-1}, and resulting in a shift towards higher wavenumbers. This effect was more pronounced in samples treated in the form of flour compared to grain, with the exception of buckwheat, which exhibited a different trend consistent with the molecular and functional modifications (see Sections 3.1 and 3.5). Among the matrices, amaranth showed the most pronounced modifications, while sorghum exhibited the least. The greater structural disruption observed in flour samples aligns with findings from Section 3.1, where increased susceptibility to hydrolysis of amylose and amylopectin was reported in flour-treated samples. These variations on the IR spectra could be related to a partial starch gelatinization, as previously described in the literature [42].

3.3. X-ray diffraction pattern and relative crystallinity

The relative crystallinity of the samples, calculated from the diffraction patterns, is presented in Table 2, with the corresponding graphs provided in Fig. 4. All the samples exhibited an orthorhombic crystal structure, which is commonly found in A-type in starches, having the main diffraction peaks as reported by Rodriguez-Garcia et al. [44], and shown in Fig. 4. This crystal structure is characteristic of cereals and pseudocereals, as previously reported by other authors for these untreated matrices [4,10,44]. The orthorhombic crystal structure was maintained after treatment, with only slight variations observed in peak intensities. The calculated relative crystallinity significantly varied among matrices ($p < 0.001$) but was not significantly affected by the treatment applied ($p > 0.05$) (Table 2). Despite the partial gelatinization observed after MWT of these four matrices [5], no significant changes in relative crystallinity were detected. This finding aligns with those previously reported by our research group, in which the MWT of buckwheat grains [21], quinoa grains [20], and rice flour [15] at high MC (20–30 %) caused only minor, generally non-significant, changes in relative crystallinity. To further evaluate the effect of MWT on the crystalline structure, the relationship between specific crystal planes was analysed by calculating the intensity ratios $I_{(031)}/I_{(231)}$ and $I_{(031)}/I_{(040)}$, as proposed by Rojas-Molina et al. [45]. These results are presented in Table 2. The ratio $I_{(031)}/I_{(231)}$ remained unaffected by the MWT, whereas the ratio $I_{(031)}/I_{(040)}$ was significantly reduced in all matrices, showing a 5–9 % decrease depending on the matrix and treatment conditions. These results further confirm that slight modifications to the crystal structure occur following MWT, but their magnitude is limited.

3.4. CLSM observations

The shape and distribution of starch and protein in the flours were examined using CLSM. The resulting 3D confocal micrographs illustrate the distribution of proteins (green) and polysaccharides (red) in all the samples studied (Fig. 5). The appearance of the untreated samples varied. Buckwheat and sorghum displayed starch granules encompassed by a protein matrix. This observation is consistent with the findings of Choi et al. [46], who reported starch granules of 5–30 µm and protein bodies of ~2 µm (within the limits of our micrograph resolution) in CSLM

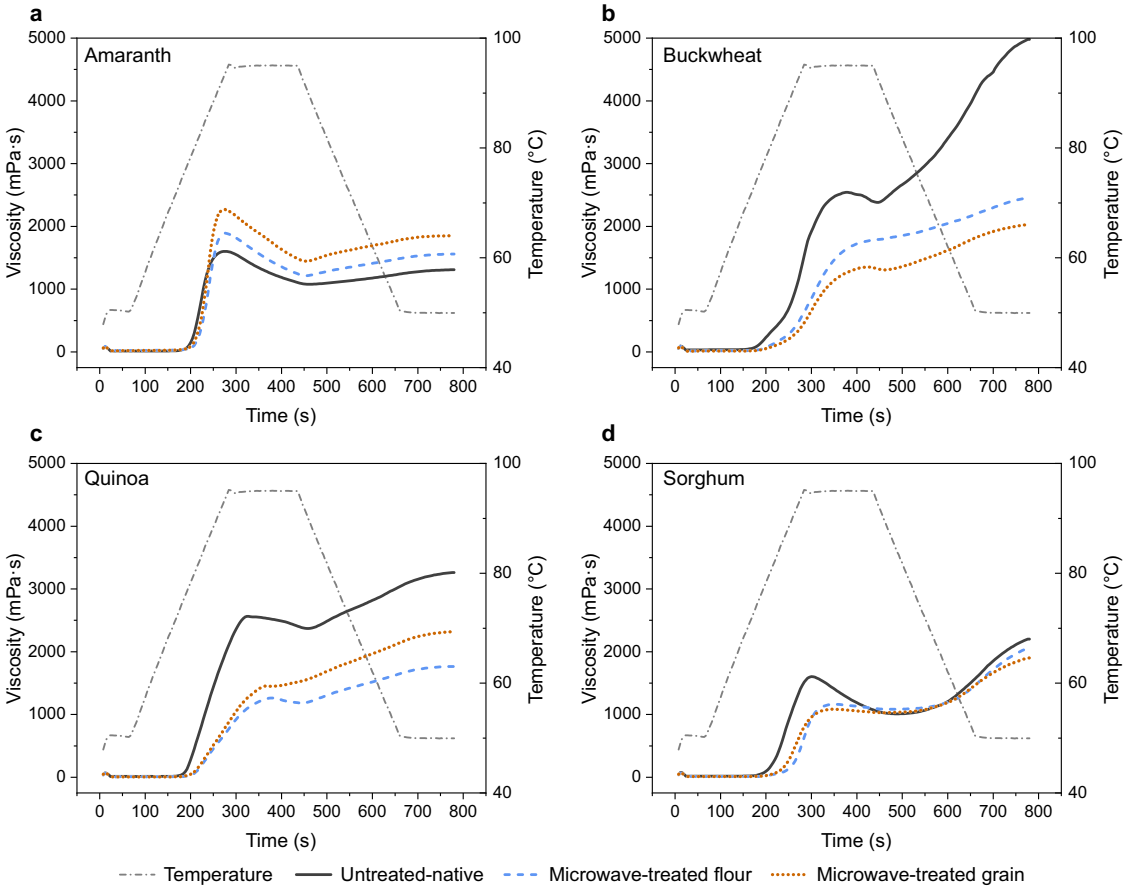

Fig. 6. Pasting profiles of amaranth (a), buckwheat (b), quinoa (c), and sorghum (d). Untreated-native flour (black, continuous line), microwave-treated flour (blue, dashed line), and microwave-treated grain (orange, dotted line) samples. The temperature profile is plotted on the second axis (grey, dash-dotted line).

Table 3
Pasting profiles of flour samples obtained from untreated and microwave-treated flours and grains.

Sample	PT (°C)	PV (mPa·s)	Pt (min)	TV (mPa·s)	BV (mPa·s)	FV (mPa·s)	SV (mPa·s)
UN-A	76.9 ± 0.5 a	1603 ± 23 a	4.58 ± 0.04 a	1078 ± 19 a	525 ± 9 a	1310 ± 10 a	232 ± 12 a
TF-A	79.7 ± 0.5 c	1894 ± 7 b	4.58 ± 0.04 a	1215 ± 18 b	679 ± 23 b	1560 ± 4 b	344 ± 15 b
TG-A	78.3 ± 0.1 b	2271 ± 46 c	4.55 ± 0.04 a	1447 ± 11 c	824 ± 36 c	1851 ± 30 c	404 ± 20 c
UN-B	74.7 ± 0.5 a	2545 ± 45 c	6.30 ± 0.04 a	2382 ± 77 c	163 ± 33 b	4980 ± 28 c	2599 ± 105 b
TF-B	84.9 ± 0.8 b	1782 ± 67 b	7.27 ± 0.01 b	1782 ± 67 b	0 ± 0 a	2455 ± 108 b	673 ± 67 a
TG-B	88.3 ± 0.3 c	1361 ± 8 a	7.04 ± 0.21 b	1306 ± 34 a	55 ± 35 a	2031 ± 38 a	725 ± 72 a
UN-Q	75.3 ± 0.3 a	2567 ± 27 c	5.44 ± 0.08 a	2370 ± 41 c	198 ± 15 c	3263 ± 31 c	893 ± 21 b
TF-Q	80.5 ± 0.5 c	1272 ± 4 a	6.33 ± 0.14 c	1183 ± 6 a	89 ± 9 b	1765 ± 17 a	582 ± 12 a
TG-Q	79.4 ± 0.5 b	1453 ± 12 b	6.09 ± 0.03 b	1445 ± 18 b	8 ± 7 a	2318 ± 29 b	873 ± 14 b
UN-S	78.2 ± 0.1 a	1605 ± 3 c	5.23 ± 0.40 a	1011 ± 14 a	594 ± 16 c	2201 ± 16 c	1190 ± 25 c
TF-S	88.1 ± 0.1 c	1162 ± 1 b	5.80 ± 0.01 b	1084 ± 4 b	78 ± 5 b	2054 ± 22 b	970 ± 26 b
TG-S	84.8 ± 0.1 b	1083 ± 11 a	5.78 ± 0.04 b	1028 ± 9 a	55 ± 2 a	1901 ± 17 a	873 ± 19 a
Analysis of variance and significance (p-values)							
Matrix (F1)	***	***	***	***	***	***	***
Treatment (F2)	***	***	***	***	***	***	***
F1 × F2	***	***	***	***	***	***	***

Flours obtained from untreated-native (UN), microwave-treated grain (TG), and microwave-treated flour (TF) samples of amaranth (A), buckwheat (B), quinoa (Q), and sorghum (S). PT: pasting temperature, PV: peak viscosity, Pt: peak time, TV: trough viscosity, BV: breakdown viscosity, FV: final viscosity, SV: setback viscosity. Data are expressed as mean ± standard deviation. Significant statistical differences ($p < 0.05$) are indicated by different letters for the same parameter and matrix. Analysis of variance and significance of matrix (A,B,Q,S), treatment (UN, TG, TF), and their interaction: ***$p < 0.001$, **$p < 0.01$, *$p < 0.05$, ns: non-significant.

images of sorghum. Untreated amaranth and quinoa showed smaller starch granules, with a size of 0.5–2 μm, as reported by Perez-Rea & Antezana-Gomez [47]. The starch granules of quinoa and amaranth were challenging to discern at the magnification employed, particularly when they were presented as compact agglomerates that appeared to constitute a single, larger structure. Furthermore, protein, which has an average particle size of approximately 200 nm for quinoa [40], was concentrated in specific areas and exhibited a less uniform distribution around starch granules than in sorghum or buckwheat.

After MWT, the starch granules of amaranth and quinoa were less

distinguishable, especially in the flour treatment. The small individual red dots observed in the native samples changed to more diffuse red aggregates. This effect was less pronounced for the larger starch granules of sorghum and buckwheat. The shape varied slightly in treated samples, appearing more rounded and less polygonal compared to native starch granules. These modifications may be related to the partial pasting of starch granules with amylose exudation, as has been commonly reported after MWT [15,16]. Regarding the protein effect after MWT, the green protein spots became more dispersed, forming a fused network surrounding starch in buckwheat and sorghum, and appearing as fused groups in amaranth and quinoa, particularly after flour treatment. Other authors have previously reported the occurrence of protein aggregation and denaturation after MWT of flour and grain samples [15,16,20]. These results are consistent with the increased disorder observed in protein secondary structure analysis using FTIR. The unfolded and/or denatured proteins, with more reactive groups exposed, may disperse and adhere between them and to the starch granules, contributing to the formation of protein and protein-starch agglomerates [16,40].

3.5. Pasting properties

Fig. 6 presents the pasting profiles of the studied flours, while Table 3 lists the resulting pasting parameters. The matrix, treatment, and their interaction (matrix × treatment) had a significant effect ($p < 0.001$) on all pasting parameters.

The viscosity profiles of untreated flours from different botanical origins were found to be significantly different (Fig. 5), which is in line with the profiles reported in previous studies in untreated amaranth, buckwheat, quinoa, and sorghum flours [3,10]. MWT had a differential impact on the various matrices, resulting in diverse modifications in the pasting profiles. Amaranth exhibited higher pasting profiles after MWT, whereas buckwheat, quinoa, and sorghum showed lower pasting profiles. The only common modification for all microwave-treated flours and grains was an increase in pasting temperature. This increase was greater for flour than for grain treatments, except for buckwheat. A delayed pasting temperature following thermal treatment has been associated with the formation of cross-linkages within starch granules and a reduction in swelling power, which results in greater heat required for disintegration of the starch structure and paste formation [19,48].

The peak, trough, breakdown, final, and setback viscosities of buckwheat, quinoa, and sorghum were lower in the treated flours than those in the corresponding untreated flours. This behaviour has been the most frequently reported for the MWT of starch [12]. The reduced peak viscosity indicates a decreased swelling capacity of the starch granules [10]. Thermal degradation of amylopectin and amylose during heating may be responsible for the lower peak viscosity [23]. Moreover, a lower breakdown indicates higher stability of the swollen granules towards heating and shearing [19]. However, between the grain and flour treatments, the changes were not in the same direction for all the matrices. Buckwheat and sorghum showed lower viscosity profiles for the grain treatment than for the flour treatment, although the relative differences were much lower in sorghum than in buckwheat. Nevertheless, in the case of quinoa, the reduction in pasting profile was more pronounced in the flour treatment than in the grain treatment. The observed differences between the grain and flour treatments of these matrices may be related to the different sizes and compositions of seeds. This was particularly evident in the starch granules and protein characteristics, as previously discussed.

Amaranth demonstrated a notable increase in peak, trough, breakdown, final, and setback viscosities in treated flours compared with untreated flours. These modifications were greater in the grain treatment than in the flour treatment. For example, the peak viscosity increased from 1603 mPa·s for UN-A to 1894 mPa·s for TF-A and 2271 mPa·s for TG-A. This behaviour is similar to that observed for hydrothermal treatment of amaranth grains with a steamer atmospheric pressure and at a temperature of 99 °C for 3, 6, and 9 min [49]. These authors observed that the peak, trough, and breakdown viscosities of amaranth flour were higher after treatment. In our study, the starch and protein of amaranth were among of the most modified after MWT, although these modifications were in line with those observed for the other matrices, which exhibited lowered viscosimetric profiles. The different effects, with enhanced pasting profiles after MWT, may be related to the molecular structure of amaranth, which exhibited the most compact structure among the studied samples. MWT may have caused partial disruption of the cell walls, facilitating access to water in the granules and increasing their swelling capacity [50], leading to a higher peak viscosity. In addition, it has been reported that an extensive hydrolysis with the formation of small fragments is more likely to decrease the paste viscosity [51]. Nevertheless, the MWT of amaranth

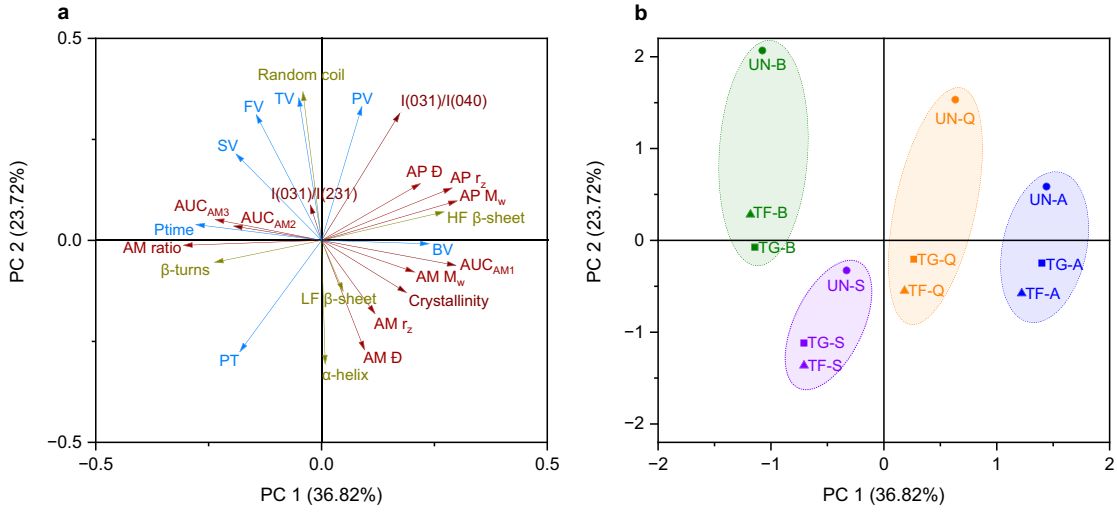

Fig. 7. Principal component analysis (PCA) showing (a) the studied parameters (starch-related properties are shown in red, protein-related properties in green, and pasting properties in blue) and (b) the sample scores. Parameters are represented as: AM (amylose), AP (amylopectin), M_w (weight-average molar mass), r_z (z-average root-mean-square radius), Đ (dispersity), AUC_{AM1}, AUC_{AM2}, AUC_{AM3} (percentual areas under the amylose peak corresponding to short, intermediate, and long amylose chains, respectively), I(031)/I(231) and I(031)/I(040) (intensity ratios of XRD), LF (low frequency), HF (high frequency), PT (pasting temperature), PV (peak viscosity), Ptime (peak time), TV (trough viscosity), BV (breakdown viscosity), FV (final viscosity), and SV (setback viscosity). Samples are labelled as follows: untreated native flour (UN), microwave-treated grain (TG), and microwave-treated flour (TF) from amaranth (A), buckwheat (B), quinoa (Q), and sorghum (S).

produces amylopectin fragments of high molecular weight, as explained in Section 3.1. Therefore, this particularity in the amaranth structure and its modification with MWT may explain its different behaviour compared to the other matrices, resulting in a higher pasting profile after MWT, particularly when treated in flour form. However, the modification of other flour components, such as lipids or fibre, during the MWT may have also influenced the differences in the pasting profiles.

3.6. Principal component analysis

Principal component analysis (PCA) was employed to further describe the correlation between the measured properties and the effects of MWT, depending on the matrix and treatment form (Fig. 7). The statistical model explained 60.54 % of the total variation, with the first principal component (PC1) accounting for 36.82 % and the second principal component (PC2) explaining 23.72 %.

The loadings of the parameters on PC1 and PC2 (Fig. 7a) revealed distinct contributions of starch-related (red), protein-related (yellow), and pasting (blue) properties. PC1 was primarily influenced by starch-related parameters, with strong positive loadings for amylopectin weight and size (AP M_w and AP r_z) as well as the proportion of short amylose chains (AUC_{AM1}). Conversely, negative loadings were observed for amylose ratio (AM ratio), and proportion of medium and long amylose chains (AUC_{AM2} and AUC_{AM3}, respectively). The XRD parameters of $I_{(031)}/I_{(040)}$ and crystallinity also influenced PC1, showing strong positive loadings. PC2 was strongly influenced protein secondary structure, and pasting properties. Among protein-related parameters, random coil displayed the strongest positive loading, whereas α-helix had the strongest negative contribution to PC2. Pasting properties, including trough viscosity (TV), peak viscosity (PV), final viscosity (FV), breakdown viscosity (BV), and setback viscosity (SV), exhibited strong positive loadings, whereas pasting temperature (PT) had a strong negative contribution. These results suggest that PC1 primarily captures the structural modifications in starch molecules induced by MWT, whereas PC2 reflects the alterations in protein secondary structure and flour pasting behaviour.

The PCA score plot (Fig. 7b) revealed that native samples were distributed in distinct quadrants, reflecting differences in structural and functional properties based on botanical origin. Notably, amaranth and quinoa clustered in the same quadrant, suggesting similar structural characteristics due to their closer botanical relationship.

MWT induced consistent shifts in the PCA score plot, with all treated samples moving towards lower PC1 and PC2 scores (Fig. 7b), indicating systematic modifications across all samples, regardless of their original properties. The samples exhibited the following modification pattern, from most to least modified in terms of the Euclidean distances between untreated and treated samples: TG-B > TF-Q > TF-B > TG-Q > TF-A > TF-S > TG-S > TG-A. Notably, the reduction in PC2 was more pronounced than that in PC1 for all treated samples. The reduction in PC1 scores aligns with the observed hydrolysis of amylopectin (lower AP M_w and AP r_z) and lower $I_{(031)}/I_{(040)}$ due to MWT. For PC2, the reductions could be associated with the overall decrease in pasting profiles (lower PV, TV, FV), the lower $I_{(031)}/I_{(040)}$, and the increases in PT. MWT increases the disorder in protein secondary structure, as evidenced by reductions in α-helix content and increases in random coil content. However, the position of the samples in the score plot aligns oppositely to what is expected from these vectors, indicating that changes in protein secondary structure have a smaller impact on the overall effect of MWT compared to the molecular structure of starch and the pasting properties. The shifts in the PCA plot were more pronounced for MWT flour than for MWT grain, except for buckwheat. TG-B showed a greater reduction in PC2 score than TF-B. This behaviour is likely due to the lower pasting profile of TF-B compared to that of TG-B which contrasts with the general trend observed in other samples.

Overall, these results demonstrate that MWT induces similar effects across all samples, regardless of their initial structural properties, under identical treatment conditions. However, the extent of modification is influenced by the botanical origin of the samples and whether the treatment was applied on grain or flour. This underscores the interplay between sample characteristics and treatment form in determining the structural and functional outcomes of MWT.

4. Conclusions

This study on the effects of MWT highlights the significant influence of botanical origin (amaranth, buckwheat, quinoa, or sorghum) and form of treatment (grain or flour) on the molecular structure of starch and protein and the pasting properties of the resulting flours. MANOVA showed that extent of change in most of the parameters studied depended on the matrix, the form of treatment (grain or flour), and their interaction (matrix × treatment). MWT consistently caused partial fragmentation of the amylose and amylopectin chains, with amylopectin being more susceptible to hydrolysis than amylose, particularly at α-(1 → 6) glycosidic linkages. Nevertheless, the granular crystalline structure was largely preserved, suggesting that the structural changes occurred predominantly in the amorphous regions. MWT altered the morphology of the starch granules so that they were less angular and more swollen, probably due to partial gelatinisation and amylose leaching. These changes were accompanied by a more disordered protein secondary structure, possibly allowing greater exposure of reactive groups. The flour treatments resulted in more pronounced effects than grain treatments across all matrices (with the exception of buckwheat for some properties), likely due to the removal of the grain outer layers that protect starch granules during milling, which allows for greater molecular mobility and interaction during MWT. Among the matrices studied, amaranth exhibited the greatest change after MWT, showing widespread disruption of both starch and protein structures. The greater susceptibility to treatment-induced hydrolysis of starch in the amaranth samples was attributed to the low amylose content and large amylopectin size. In contrast, buckwheat showed the least structural change, while quinoa and sorghum showed intermediate behaviour. These differences in resistance to modification are probably due to differences in the organization of starch granules and protein characteristics. The extent of microwave-induced changes in the pasting properties of the flours varied according to their intrinsic properties along with the observed structural changes. PCA analysis confirmed all these observations and showed consistent structural changes in all matrices, regardless of their intrinsic properties. Overall, the results of this study provide novel insights into the effects of MWT on different matrices in grain and flour forms, thereby enabling a more profound understanding of the structure/function relationship in MWT.

Supplementary data to this article can be found online at https://doi.org/10.1016/j.ijbiomac.2025.145094.

CRediT authorship contribution statement

Ainhoa Vicente: Writing – review & editing, Writing – original draft, Visualization, Methodology, Investigation, Formal analysis, Conceptualization. **Raúl R. Mauro:** Writing – review & editing, Methodology, Formal analysis. **Marina Villanueva:** Visualization, Validation, Methodology, Conceptualization. **Pedro A. Caballero:** Supervision, Resources, Methodology, Conceptualization. **Bruce Hamaker:** Writing – review & editing, Supervision, Resources, Methodology. **Felicidad Ronda:** Writing – review & editing, Validation, Supervision, Resources, Project administration, Methodology, Funding acquisition, Conceptualization.

Declaration of competing interest

The authors confirm that they have nothing to declare.

Data availability

Data will be made available on request.

Acknowledgements

The authors thank the Spanish Ministerio de Ciencia e Innovación (PID2019-110809RB-I00 and EQC2021-006985-P), Ministerio de Ciencia, Innovación y Universidades (PID2023-153330OB-I00) and the Junta de Castilla y León/FEDER (VA195P20 and CLU 2019-04 – BIO-ECOUVA Unit of Excellence of the University of Valladolid) for their financial support. A. Vicente thanks the Spanish Ministerio de Ciencia, Innovación y Universidades for her FPU doctorate grant and R. Mauro for his predoctoral contract. A. Vicente thanks IMFAHE Foundation for the Excellence Fellowship.

References

[1] A. Khoddami, V. Messina, K. Vadabalija Venkata, A. Farahnaky, C.L. Blanchard, T. H. Roberts, Sorghum in foods: functionality and potential in innovative products, Crit. Rev. Food Sci. Nutr. 63 (2023) 1170–1186, https://doi.org/10.1080/10408398.2021.1960793.

[2] H. Yong, X. Wang, J. Sun, Y. Fang, J. Liu, C. Jin, Comparison of the structural characterization and physicochemical properties of starches from seven purple sweet potato varieties cultivated in China, Int. J. Biol. Macromol. 120 (2018) 1632–1638, https://doi.org/10.1016/j.ijbiomac.2018.09.182.

[3] P. De Bock, L. Daelemans, L. Selis, K. Raes, P. Vermeir, M. Eeckhout, F. Van Bockstaele, Comparison of the chemical and technological characteristics of wholemeal flours obtained from amaranth (*Amaranthus* sp.), quinoa (*Chenopodium quinoa*) and guckwheat (*Fagopyrum* sp.) seeds, Foods 10 (2021) 651, https://doi.org/10.3390/foods10030651.

[4] C. Fuentes, D. Perez-Rea, B. Bergenståhl, S. Carballo, M. Sjöö, L. Nilsson, Physicochemical and structural properties of starch from five Andean crops grown in Bolivia, Int. J. Biol. Macromol. 125 (2019) 829–838, https://doi.org/10.1016/j.ijbiomac.2018.12.120.

[5] A. Vicente, M. Villanueva, J.M. Muñoz, P.A. Caballero, F. Ronda, The role of microwave absorption capacity and water mobility in the microwave treatment of grain vs. flour: impact on the treated flour characteristics, Food Hydrocoll. 159 (2025) 110680, https://doi.org/10.1016/j.foodhyd.2024.110680.

[6] C. Martínez-Villaluenga, E. Peñas, B. Hernández-Ledesma, Pseudocereal grains: nutritional value, health benefits and current applications for the development of gluten-free foods, Food Chem. Toxicol. 137 (2020) 111178, https://doi.org/10.1016/j.fct.2020.111178.

[7] Y. Zhao, D. Tu, D. Wang, J. Xu, W. Zhuang, F. Wu, Y. Tian, Structural and property changes of starch derivatives under microwave field: a review, Int. J. Biol. Macromol. 256 (2024) 128465, https://doi.org/10.1016/j.ijbiomac.2023.128465.

[8] Q. Bao, M. Li, K. Yang, Y. Lv, S. Ma, Effect of highland barley treated with heat–moisture on interactions between gluten and starch granules in dough, Int. J. Biol. Macromol. 275 (2024), https://doi.org/10.1016/j.ijbiomac.2024.133254.

[9] K. Schafranski, V.C. Ito, L.G. Lacerda, Impacts and potential applications: a review of the modification of starches by heat-moisture treatment (HMT), Food Hydrocoll. 117 (2021) 106690, https://doi.org/10.1016/j.foodhyd.2021.106690.

[10] Q. Sun, Z. Han, L. Wang, L. Xiong, Physicochemical differences between sorghum starch and sorghum flour modified by heat-moisture treatment, Food Chem. 145 (2014) 756–764, https://doi.org/10.1016/j.foodchem.2013.08.129.

[11] C. Collar, Significance of heat-moisture treatment conditions on the pasting and gelling behaviour of various starch-rich cereal and pseudocereal flours, Food Sci. Technol. Int. 23 (2017) 623–636, https://doi.org/10.1177/1082013217714671.

[12] M. Yi, X. Tang, S. Liang, R. He, T. Huang, Q. Lin, R. Zhang, Effect of microwave alone and microwave-assisted modification on the physicochemical properties of starch and its application in food, Food Chem. 446 (2024) 138841, https://doi.org/10.1016/j.foodchem.2024.138841.

[13] Y. Tian, Y. Wang, K. Herbuger, B.L. Petersen, Y. Cui, A. Blennow, X. Liu, Y. Zhong, High-pressure pasting performance and multilevel structures of short-term microwave-treated high-amylose maize starch, Carbohydr. Polym. 322 (2023) 121366, https://doi.org/10.1016/j.carbpol.2023.121366.

[14] R.A. Cave, S.A. Seabrook, M.J. Gidley, R.G. Gilbert, Characterization of starch by size-exclusion chromatography: the limitations imposed by shear scission, Biomacromolecules 10 (2009) 2245–2253, https://doi.org/10.1021/bm900426n.

[15] Á.G. Solaesa, M. Villanueva, A.J. Vela, F. Ronda, Impact of microwave radiation on in vitro starch digestibility, structural and thermal properties of rice flour. From dry to wet treatments, Int. J. Biol. Macromol. 222 (2022) 1768–1777, https://doi.org/10.1016/j.ijbiomac.2022.09.262.

[16] N. An, D. Li, L. Wang, Y. Wang, Microwave irradiation of corn kernels: effects on structural, thermal, functional and rheological properties of corn flour, Food Hydrocoll. 143 (2023) 108939, https://doi.org/10.1016/j.foodhyd.2023.108939.

[17] A. Kheto, D. Joseph, M. Islam, S. Dhua, R. Das, Y. Kumar, R. Vashishth, V. S. Sharanagat, K. Kumar, P.K. Nema, Microwave roasting induced structural, morphological, antioxidant, and functional attributes of quinoa (*Chenopodium quinoa* Willd), J. Food Process. Preserv. 46 (2022) e16595, https://doi.org/10.1111/jfpp.16595.

[18] M.V. Rao, C.K. Sunil, N. Venkatachalapathy, Effect of microwave and hot air radiofrequency treatments on physicochemical and functional properties of foxtail millet flour and its protein isolate, J. Cereal Sci. 114 (2023) 103774, https://doi.org/10.1016/j.jcs.2023.103774.

[19] Á.G. Solaesa, M. Villanueva, J.M. Muñoz, F. Ronda, Dry-heat treatment vs. heat-moisture treatment assisted by microwave radiation: techno-functional and rheological modifications of rice flour, LWT 141 (2021) 110851, https://doi.org/10.1016/j.lwt.2021.110851.

[20] A. Vicente, M. Villanueva, P.A. Caballero, J.M. Muñoz, F. Ronda, Microwave modification of quinoa grains at constant and varying water content modulates changes in structural and physico-chemical properties of the resulting flours, Foods 12 (2023) 1421, https://doi.org/10.3390/foods12071421.

[21] A. Vicente, M. Villanueva, P.A. Caballero, J.M. Muñoz, F. Ronda, Buckwheat grains treated with microwave radiation: impact on the techno-functional, thermal, structural, and rheological properties of flour, Food Hydrocoll. 137 (2023) 108328, https://doi.org/10.1016/j.foodhyd.2022.108328.

[22] Z.A. Syahariza, E. Li, J. Hasjim, Extraction and dissolution of starch from rice and sorghum grains for accurate structural analysis, Carbohydr. Polym. 82 (2010) 14–20, https://doi.org/10.1016/j.carbpol.2010.04.014.

[23] A.K. Anderson, H.S. Guraya, Effects of microwave heat-moisture treatment on properties of waxy and non-waxy rice starches, Food Chem. 97 (2006) 318–323, https://doi.org/10.1016/j.foodchem.2005.04.025.

[24] G.C. Berry, Thermodynamic and conformational properties of polystyrene. I. Light-scattering studies on dilute solutions of linear polystyrenes, J. Chem. Phys. 44 (1966) 4550–4564, https://doi.org/10.1063/1.1726673.

[25] S. Chakraborty, B. Sahoo, I. Teraoka, R.A. Gross, Solution properties of starch nanoparticles in water and DMSO as studied by dynamic light scattering, Carbohydr. Polym. 60 (2005) 475–481, https://doi.org/10.1016/J.CARBPOL.2005.03.011.

[26] A.J. Vela, M. Villanueva, C. Li, B. Hamaker, F. Ronda, Ultrasound treatments of tef [Eragrostis tef (Zucc.) trotter] flour rupture starch α-(1,4) bonds and fragment amylose with modification of gelatinization properties, LWT 174 (2023) 114463, https://doi.org/10.1016/j.lwt.2023.114463.

[27] M.M. Martinez, C. Li, M. Okoniewska, I. Mukherjee, D. Vellucci, B. Hamaker, Slowly digestible starch in fully gelatinized material is structurally driven by molecular size and A and B1 chain lengths, Carbohydr. Polym. 197 (2018) 531–539, https://doi.org/10.1016/j.carbpol.2018.06.021.

[28] F. Vilaplana, R.G. Gilbert, Characterization of branched polysaccharides using multiple-detection size separation techniques, J. Sep. Sci. 33 (2010) 3537–3554, https://doi.org/10.1002/jssc.201000525.

[29] O.K. Ozturk, S.G. Kaasgaard, L.G. Palmén, B.C. Vidal, B.R. Hamaker, Enzyme treatments on corn fiber from wet-milling process for increased starch and protein extraction, Ind. Crop. Prod. 168 (2021) 113622, https://doi.org/10.1016/j.indcrop.2021.113622.

[30] M. Fevzioglu, O.K. Ozturk, B.R. Hamaker, O.H. Campanella, Quantitative approach to study secondary structure of proteins by FT-IR spectroscopy, using a model wheat gluten system, Int. J. Biol. Macromol. 164 (2020) 2753–2760, https://doi.org/10.1016/j.ijbiomac.2020.07.299.

[31] D.M. Byler, H. Susi, Examination of the secondary structure of proteins by deconvolved FTIR spectra, Biopolymers 25 (1986) 469–487, https://doi.org/10.1002/bip.360250307.

[32] Y. Vodovotz, P. Chinachoti, Confocal microscopy of bread, in: New Techniques in the Analysis of Foods, Springer US, Boston, MA, 1998, pp. 9–17, https://doi.org/10.1007/978-1-4757-5995-2_2.

[33] T. Bantan-Polak, M. Kassai, K.B. Grant, A comparison of fluorescamine and naphthalene-2,3-dicarboxaldehyde fluorogenic reagents for microplate-based detection of amino acids, Anal. Biochem. 297 (2001) 128–136, https://doi.org/10.1006/abio.2001.5338.

[34] AACC, Approved Methods of Analysis, 11th ed., 2010. St. Paul, MN, U.S.A.

[35] X. Xu, Y. Chen, Z. Luo, X. Lu, Different variations in structures of A- and B-type starches subjected to microwave treatment and their relationships with digestibility, LWT 99 (2019) 179–187, https://doi.org/10.1016/j.lwt.2018.09.072.

[36] Q. Yang, L. Qi, Z. Luo, X. Kong, Z. Xiao, P. Wang, X. Peng, Effect of microwave irradiation on internal molecular structure and physical properties of waxy maize starch, Food Hydrocoll. 69 (2017) 473–482, https://doi.org/10.1016/j.foodhyd.2017.03.011.

[37] K. Wang, P.W. Wambugu, B. Zhang, A.C. Wu, R.J. Henry, R.G. Gilbert, The biosynthesis, structure and gelatinization properties of starches from wild and cultivated African rice species (Oryza barthii and Oryza glaberrima), Carbohydr. Polym. 129 (2015) 92–100, https://doi.org/10.1016/j.carbpol.2015.04.035.

[38] Z. Gu, G. Cheng, X. Sha, H. Wu, X. Wang, R. Zhao, Q. Huang, Y. Feng, J. Tang, H. Jiang, Heat-moisture treatment of freshly harvested high-amylose maize kernels improves its starch thermal stability and enzymatic resistance, Carbohydr. Polym. 340 (2024) 122303, https://doi.org/10.1016/j.carbpol.2024.122303.

[39] Q. Bao, J. Yan, Z. Wang, S. Ma, Changes in the structure and aggregation behavior of wheat glutenin and gliadin induced by the combined action of heat treatment and wheat bran dietary fiber, Food Hydrocoll. 148 (2024) 109506, https://doi.org/10.1016/j.foodhyd.2023.109506.

[40] K. Huang, J. Shi, M. Li, R. Sun, W. Guan, H. Cao, X. Guan, Y. Zhang, Intervention of microwave irradiation on structure and quality characteristics of quinoa protein aggregates, Food Hydrocoll. 130 (2022) 107677, https://doi.org/10.1016/j.foodhyd.2022.107677.

[41] A. Vicente, M. Villanueva, P.A. Caballero, A. Lazaridou, C.G. Biliaderis, F. Ronda, Flours from microwave-treated buckwheat grains improve the physical properties

and nutritional quality of gluten-free bread, Food Hydrocoll. 149 (2024) 109644, https://doi.org/10.1016/j.foodhyd.2023.109644.
[42] G. Velazquez, C.F. Ramirez-Gutierrez, G. Mendez-Montealvo, R. Velazquez-Castillo, L.F. Morelos-Medina, E. Morales-Sánchez, M. Gaytán-Martínez, M. E. Rodríguez-García, B. Contreras-Jiménez, Effect of long-term retrogradation on the crystallinity, vibrational and rheological properties of potato, corn, and rice starches, Food Chem. 477 (2025) 143455, https://doi.org/10.1016/j.foodchem.2025.143455.
[43] F.J. Warren, M.J. Gidley, B.M. Flanagan, Infrared spectroscopy as a tool to characterise starch ordered structure—a joint FTIR–ATR, NMR, XRD and DSC study, Carbohydr. Polym. 139 (2016) 35–42, https://doi.org/10.1016/J.CARBPOL.2015.11.066.
[44] M.E. Rodriguez-Garcia, M.A. Hernandez-Landaverde, J.M. Delgado, C.F. Ramirez-Gutierrez, M. Ramirez-Cardona, B.M. Millan-Malo, S.M. Londoño-Restrepo, Crystalline structures of the main components of starch, Curr. Opin. Food Sci. 37 (2021) 107–111, https://doi.org/10.1016/J.COFS.2020.10.002.
[45] I. Rojas-Molina, M.G. Nieves-Hernandez, E. Gutierrez-Cortez, O.Y. Barrón-García, M. Gaytán-Martínez, M.E. Rodriguez-Garcia, Physicochemical changes in starch during the conversion of corn to tortilla in the traditional nixtamalization process associated with RS2, Food Chem. 439 (2024) 138088, https://doi.org/10.1016/j.foodchem.2023.138088.
[46] S.J. Choi, H.D. Woo, S.H. Ko, T.W. Moon, Confocal laser scanning microscopy to investigate the effect of cooking and sodium bisulfite on in vitro digestibility of waxy sorghum flour, Cereal Chem. 85 (2008) 65–69, https://doi.org/10.1094/CCHEM-85-1-0065.
[47] D. Perez-Rea, R. Antezana-Gomez, The functionality of pseudocereal starches, in: Starch in Food, Elsevier, 2018, pp. 509–542, https://doi.org/10.1016/B978-0-08-100868-3.00012-3.
[48] M. Siwatch, R.B. Yadav, B.S. Yadav, Annealing and heat-moisture treatment of amaranth starch: effect on structural, pasting, and rheological properties, J. Food Meas. Charact. 16 (2022) 2323–2334, https://doi.org/10.1007/s11694-022-01325-1.
[49] A. Malik, K. Khamrui, W. Prasad, Effect of hydrothermal treatment on physical properties of amaranth, an underutilized pseudocereal, Future Foods 3 (2021) 100027, https://doi.org/10.1016/j.fufo.2021.100027.
[50] S. Reyniers, N. De Brier, S. Matthijs, K. Brijs, J.A. Delcour, Impact of physical and enzymatic cell wall opening on the release of pre-gelatinized starch and viscosity forming potential of potato flakes, Carbohydr. Polym. 194 (2018) 401–410, https://doi.org/10.1016/j.carbpol.2018.04.057.
[51] H. Li, M. Xu, S. Yan, R. Liu, Z. Ma, Y. Wen, J. Wang, B. Sun, Insights into waxy maize starch degradation by sulfuric acid: impact on starch structure, pasting, and rheological property, Int. J. Biol. Macromol. 165 (2020) 214–221, https://doi.org/10.1016/j.ijbiomac.2020.09.148.